Available online at www.sciencedirect.com

SciVerse ScienceDirect

Ceramics International 38 (2012) 3001–3009

CERAMICS INTERNATIONAL

www.elsevier.com/locate/ceramint

Influences of pH on the structure, morphology and dielectric properties of bismuth titanate ceramics produced by a low-temperature self-combustion synthesis without an additional fuel agent

Warapong Krengvirat [a,c], Srimala Sreekantan [a,*], Ahmad-Fauzi Mohd Noor [a], Charoen Chinwanitcharoen [b], Hiroyuki Muto [c], Atsunori Matsuda [c]

[a] School of Materials and Mineral Resources Engineering, Engineering Campus, Universiti Sains Malaysia, Penang 14300, Malaysia
[b] Faculty of Engineering, Burapha University, Chonburi 20131, Thailand
[c] Department of Electrical and Electronic Information Engineering, Toyohashi University of Technology, Aichi 441-8580, Japan

Received 15 March 2011; received in revised form 3 November 2011; accepted 29 November 2011
Available online 6 December 2011

Abstract

Bismuth titanate (BIT) ceramics were prepared by incorporating low-temperature self-combustion synthesis and pH modification. The pH value of the initial precursor was adjusted to 3, 5 and 7 by the addition of ammonium hydroxide (NH_4OH) with different amount. The reaction between ammonium ions (NH_4^+) and nitrate ions (NO_3^-) induced the formation of ammonium nitrate (NH_4NO_3), in turn to favor the combustion by enhancing the decomposition rate. Excessive hydroxyl ions (OH^-) at higher pH value dominated the chelating of the metal carboxylate and the metal ions, resulting in a strong hybridization between bismuth (Bi) and oxygen (O), and also the suppression of the independent volatility of Bi and bismuth oxide (Bi_2O_3). Such conditions contributed to the formation of pure BIT via the low-temperature self-combustion synthesis without the use of an additional fuel agent. A BIT ceramic with high relative density (91.35%) that exhibited a high dielectric constant of ~340 and a low dissipation factor ~0.028 was obtained by the synthesis method at the neutral condition. Furthermore, it offers ability for the use in high temperature applications up to 675 °C.

Keywords: A. Powders: chemical preparation; B. Grain size; C. Dielectric properties; D. Perovskites

1. Introduction

Bismuth titanate ($Bi_4Ti_3O_{12}$; BIT) is a ferroelectric oxide that belongs to the Aurivillius family. A unique characteristic, high Curie temperature characteristic (675 °C) brought about BIT as a promising candidate for piezoelectric devices and memory storage (FERAM) at elevated temperatures and hostile environment applications [1–4]. BIT powder is conventionally prepared through a solid-state reaction, which involves high temperature [5]. This process generally causes coarsened, aggregated particles, which leads to a poor microstructure of ceramics and eventually results in low dielectric properties [6].

Considerable efforts have therefore been devoted to attain a high-efficiency synthesis route. Various wet-chemical syntheses, such as co-precipitation [7,8], sol–gel [9,10], hydrothermal [11] and a polymeric precursor [12], appear as potential routes to overcome the drawbacks of the conventional solid-state reaction. These techniques offer remarkable ability to control the stoichiometry, particle size, structure, as well as phase purity through a chemical reaction at low temperature [8,10]. Alternatively, self-propagation combustion (SHS) has been developed, and it has become an attractive approach to prepare high purity oxide powder. In 2004, Macedo et al. [13] found that the powder obtained from SHS exhibited plate-like particles in the range of approximately 3–5 μm in size, which is five times smaller than that prepared by a solid-state reaction. Furthermore, it demonstrated a higher dielectric constant. However, the major drawbacks of SHS are the requirement of extremely high temperature and special equipment [14]. In the last decade, wet-chemical combustion has been developed by incorporating SHS

* Corresponding author. Tel.: +60 45995255; fax: +60 45941011.
E-mail addresses: srimala@eng.usm.my, warapong001@hotmail.com (S. Sreekantan).

0272-8842/$36.00
doi:10.1016/j.ceramint.2011.11.081

and wet-chemical synthesis, which can be divided into several categories, for instance sol–gel combustion [15,16], gel-combustion [17,18], emulsion combustion [19] and low-temperature combustion [20]. These methods generally require an additional fuel agent, such as glycine, citric acid and urea [18]. The use of an additional fuel agent generally contributes to the ionization of the carboxylic acid group, which greatly favors the oxidation process. However, additional fuel agent also introduces a violent reaction, due to its strong exothermic nature [18,21].

Thus, it would be beneficial to reduce the violent reaction by eliminating the use of an additional fuel agent, while retaining a high ionization of the carboxylic acid group. In 2008, Xu et al. [18] found that the pH value of a solution affected the ionization of the carboxylic acid group of citric acid, and promoted the decomposition rate. This resulted in the formation of $Ce_{0.8}Y_{0.2}O_{1.9}$ powder with fine particle size, well grain size distribution and less agglomeration. On this basis, it implies the potential of pH modification to be an alternative route to achieve the combustion synthesis without an additional fuel agent.

Besides, it is well known that pH modification significantly affects the synthesized powder characteristics [10,22]. Gu et al. [23] found that the pH value of the solution had drawn a pronounced effect on the surface morphology, as well as optical and electrical properties of a crack-free thin film prepared by sol–gel method. In 2004, Wu et al. [24] obtained NiZn ferrite that contained 5 wt% SiO_2 powder with the crystallite size of approximately 13, 16 and 25 nm by sol–gel auto combustion at pH 3, 5 and 7, respectively. Besides, Roy et al. [25] observed that the grain size of $Ba_{0.5}Sr_{0.5}TiO_3$ thin films increased from 80 nm to 120 nm by the increase of pH value from 2.4 to 4.8. This resulted in the increment of the dielectric constant from 325 to 340 and the dielectric loss from 0.036 to 0.052. Other than that, $Bi_{3.5}La_{0.5}Ti_3O_{12}$ thin films with grain size of ~208 nm was obtained from the sample prepared at pH 3, whereas a smaller grain size of ~103 nm was obtained from the one prepared at pH 9, which eventually resulted in the reduction of the dielectric constant from 112 to 80 [26]. Although the influence of pH on the formation of various materials has been investigated, how the pH influences the formation of BIT in a low-temperature self-combustion synthesis remains to be explained. Therefore, this study reports the effect of pH modification on the chemical bonding, thermal behavior, phase formation, structure and morphology of BIT powder prepared by low-temperature self-combustion synthesis. The generation of an intermediate fuel agent by incorporating NH_4OH into the nitrate precursor is discussed in detail. The correlation between the microstructure and the densification of the ceramic on the dielectric properties is also investigated.

2. Experimental procedure

Bismuth nitrate pentahydrate [$Bi(NO_3)_3{\cdot}5H_2O$, Sigma Aldrich, 98%, USA] was dissolved in 2-methoxyethanol [$CH_3OCH_2CH_2OH$, Sigma Aldrich, 99%, USA] at 40 °C. Separately, titanium isopropoxide [$Ti(OC_4H_9)_4$, Fluka, 97%, USA] was added into 2-methoxyethanol. Acetylacetone ($CH_3COCH_2COCH_3$, Merck, 99%, USA) was subsequently added into the mixture as the chelating agent. The titanium solution was then added into the bismuth solution, while being stirred continuously. The pH value of the initial nitrate precursor was found to be ~1.5, and it was adjusted to pH values of 3, 5 and 7 using an ammonium hydroxide solution (NH_4OH, Merck, 25%, USA). The precusor was then stirred for an additional 2 h. The proposed equation for the formation of the $Bi_4Ti_3O_{12}$ phase is shown in Eq. (1).

$$\begin{aligned} 4[Bi(NO_3)_3 \cdot 5H_2O_{(aq)}] + 3[Ti[OCH(CH_3)_2]_4]_{(aq)} \\ + NH_4OH_{(aq)} \rightarrow Bi_4Ti_3O_{12(s)} + 2NH_4NO_{3(g)} \\ + 31H_2O_{(g)} + 11NH_{3(g)} + 10CO_{2(g)} + 16C_{(s)} \\ + \frac{103}{2} H_{2(g)} \end{aligned} \quad (1)$$

The precursor was heated, and then evaporated at ~90 °C to form a clear-brown gel. The gel swelled, became foamy, and subsequently ignited at ~150 °C in an ambient atmosphere. A yellow flame spread rapidly, and combustion lasted for ~10 s, after that, a puffy and porous powder had formed. The flaming temperature was found to be ~260 °C. The thermal behavior was investigated by a thermo-gravimetry/differential scanning calorimetry (TGA/DSC, SETSYS Evolution; France). The chemical bonding was investigated using a Fourier transform infrared spectroscopy (FTIR, Perkin Elmer, USA). The as-combusted powder was subjected to calcination at 750 °C for 3 h, and subsequently pelletized by uniaxial pressing at ~150 MPa. The pellets were then sintered at 1150 °C for 3 h in air. The relative density was determined based on the ASTM C373-88: 1994 using an analytical balance (Satorious CP224S; Germany). The crystal structure was identified using X-ray diffraction (XRD, Bruker D8-Discovery; Germany) with Cu k_α radiation (λ = 1.54056 Å) in the range of $10^\circ \leq 2\theta \leq 90^\circ$, and further analyzed using X'Pert HighScore Plus software (PANalytical B.V.; The Netherlands). The unit cell parameters were refined using a quantitative Rietveld refinement by comparison to the International Center of Diffraction Data (ICDD). The crystallite size was determined based on the Sherrer equation. Raman measurements were taken in a backscattering configuration using a 514.55-nm monochromatic beam from an Ar^+ laser (~20 mW) that was focused on the powder. The scattered light was collected by a Raman spectrometer (Horiba Jobin-Yvon HR800UV; Japan) in the range between 1000 and 100 cm^{-1}. The morphology was observed by a field emission scanning electron microscope (FESEM, ZEISS SUPRA 35VP; Germany). The dielectric properties were measured by an impedance/grain-phase analyzer (Agilent Technology 4194A; Japan) in the frequency range of 100 Hz to 1 MHz from room temperature (~22 °C) to 700 °C, under oscillation amplitude of 1 V.

3. Results and discussion

3.1. Powder synthesis

Fig. 1 shows the IR spectra of the initial precursor with different pH values. For pH 3, the stretching vibrations of hydroxyl (−OH) group were detected at 3011 and 3140 cm^{-1}

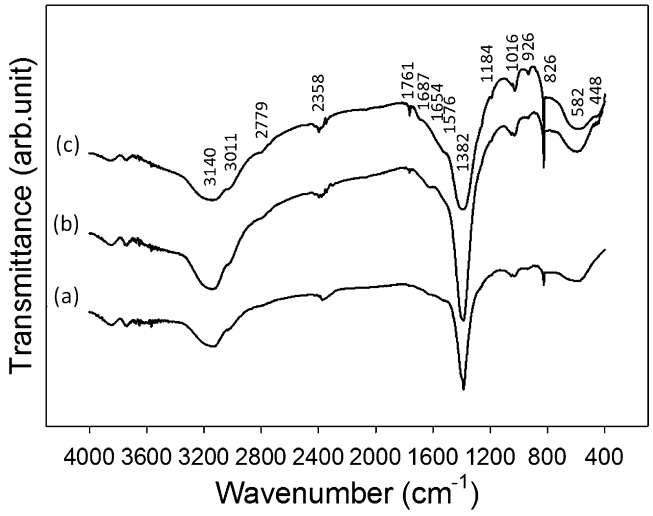

Fig. 1. IR spectra of the initial precursor prepared at (a) pH 3, (b) pH 5 and (c) pH 7.

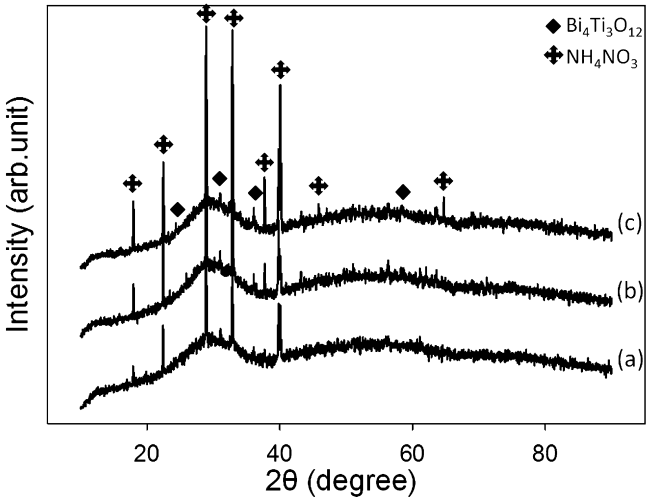

Fig. 2. XRD patterns of the initial precursor prepared at (a) pH 3, (b) pH 5 and (c) pH 7.

(Fig. 1a), corresponding to the residual water. The chelation of metal ions resulted in the formation of metal carboxylate complexes, as observed from the stretching vibration of carboxyl ions ($–COO^-$) at 1576 cm^{-1}. This is a precondition to prevent the separation or precipitation of the rare earth metal ions, and to obtain homogenous products [18]. The stretching vibrations of free –COOH group were observed at 1382, 1654 and 2358 cm^{-1}, indicating the incomplete chelation of metal ions at pH3. However, the formation of BIT is still noticeable, as manifested by the presence of perovskite unit (TiO_6) at 582 and 826 cm^{-1} [22].

The occurrence of additional transmittance bands at 1761, 1184, 926 and 448 cm^{-1} was found from the samples prepared at pH 5 and 7 (Fig. 1b and c). Moreover, the peak intensities of the bands positioned at 826 and 528 cm^{-1} were significantly increased with increasing pH value. The presence of 1761 and 926 cm^{-1} bands corresponded to a large number of OH^- ions, as verified by the stronger peak intensity of alcohol groups at 1184 and 1016 cm^{-1}. The excessive amount of OH^- ions contributed to a stronger Ti–O bond in the TiO_6 octahedron, as manifested by the stronger stretching vibrations (826 and 582 cm^{-1}) and bending vibration (448 cm^{-1}) of the TiO_6 octahedron. The band at 1576 cm^{-1} is ascribed to the asymmetric stretching of $–COO^-$ ions from the metal carboxylates, which confirmed the chelating of metal ions [18]. The increase in the peak intensity of the bands located at 2779, 1761, 1687, 1382 and 926 cm^{-1} is attributed to the higher number of –COOH groups, as a result of the reaction between the excessive OH^- ions and carbonyl group C=O [22]. This result implies that the excessive OH^- ions in nitrate precursor favors the generation of an intermediate fuel agent, due to its carboxylic-rich characteristic. The formation of an intermediate fuel agent in the precursor was further verified using XRD analysis, and the results are shown in Fig. 2.

The XRD patterns of the initial precursor revealed a large amount of the NH_4NO_3 phase, which is in agreement with the respective ICDD no. 98-2015 (Fig. 2). Additionally, a small amount of the $Bi_4Ti_3O_{12}$ phase (ICDD #98-8636) was observed. The peak intensity increased continuously with increasing the pH value, indicating the tendency to form both NH_4NO_3 and $Bi_4Ti_3O_{12}$ phases at high pH values. This is due to the fact that the additional NH_4OH content in the precursor leads to a higher number of ammonium ions (NH_4^+) and OH^- ions. The NH_4^+ ions subsequently reacted with nitrate ions (NO_3^-), and formed NH_4NO_3. At the same time, higher OH^- content reduced the number of hydrogen ions (H^+), which led to the stronger repulsion force in the Ti–O bonds. This contributed to a stronger bonding in the TiO_6 octahedron.

The effect of an intermediate NH_4NO_3 on the combustion was further investigated by the investigation of the thermal change behavior and decomposition rate (Fig. 3). A slight weight loss was detected at temperatures approximately 70–180 °C. Besides, the DTA plot shows the presence of weak endothermic peaks at approximately 70, 140 and 180 °C. These corresponded to the evaporation of the water and the organic solvent that caused heat absorption, as verified by the presence of endothermic peaks at approximately 70, 130 and 180 °C. The rapid weight loss was detected at approximately 190–270 °C. This is attributed to the decomposition of the organic materials during combustion, as confirmed by the presence of strong exothermic peaks at approximately 190, 230 and 270 °C. It is noticeable that the exothermic peak positioned at 190 °C shifted to higher temperature upon increasing pH value. Furthermore, the peak became broaden. This clearly indicates that higher intermediate fuel content could facilitate the ignition at lower temperatures. Other than that, the sample prepared at pH 5 and 7 exhibited a large weight loss of approximately 43–48%, as well as an intense exothermic peak. This is attributed to the higher decomposition rate of bismuth–titanium oxalate and the combustion of the intermediate products [21,27]. In contrary, the sample prepared at pH 3 exhibited incomplete decomposition during combustion, as revealed by the occurrence of an exothermic peak and weight loss at approximately 500–520 °C. The incomplete combustion

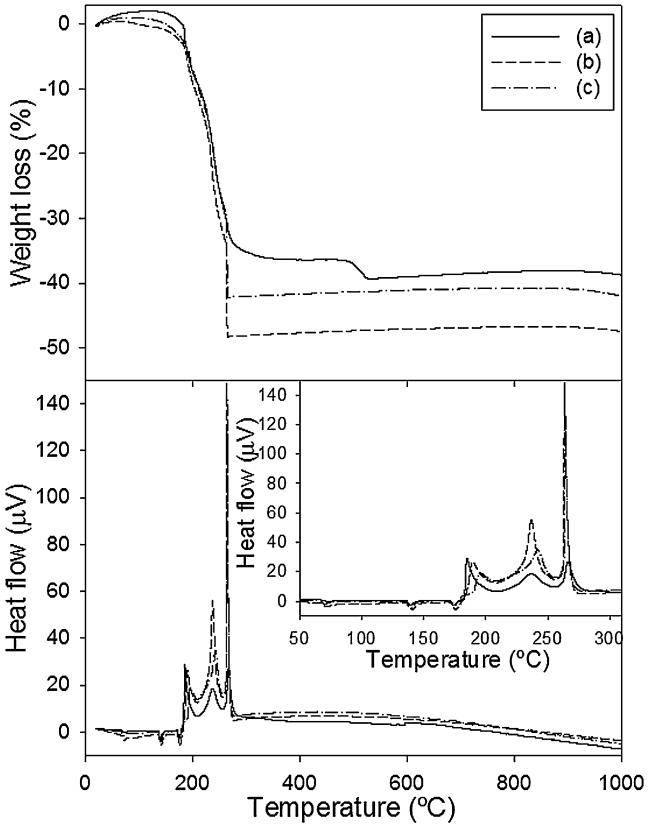

Fig. 3. TGA/DSC plots of the initial precursor prepared at (a) pH 3, (b) pH 5 and (c) pH 7.

process resulted in the residual bismuth–titanium oxalates and intermediate products. From the results, it reveals that the addition of NH_4OH in the nitrate precursor could decelerate the vaporization and favor combustion. Slow vaporization leads to a strong polymerization of the metal–oxygen bonding, and thus induces the formation of chelating complexes [25,28]. The chelating complexes consequently restrict the formation of an inorganic substance containing Ti–OH groups, which would facilitate the formation of single crystalline BIT phase [8].

The as-combusted powders were subjected to calcination at 750 °C for 3 h to eliminate the residual carbon and the unreacted organic compounds. The XRD patterns of heat-treated powders prepared at pH 5 and 7 showed the formation of the $Bi_4Ti_3O_{12}$ phase with an orthorhombic structure, which is in line with the respective ICDD no. 98-8636 (Fig. 4). However, an additional peak (3 1 0) at positioned 2θ of ~28° was found from the powder prepared at pH 3, indicating the presence of an intermediate $Bi_{12}TiO_{20}$ phase (ICDD #98-0374). Thus, it reveals that polycrystalline BIT powder can be prepared under pH of 5 and 7 conditions. The formation of $Bi_4Ti_3O_{12}$ phase was further investigated by a quantitative Rietveld analysis, and the results are summarized in Table 1.

Based on the refinement results, the samples prepared at all pH conditions exhibited an orthorhombic symmetry with the *Fmmm* space group [5,29]. The powder prepared at a pH 7 exhibited the unit cell parameters of $a = 5.408$ Å, $b = 5.446$ Å and $c = 32.814$ Å, which were confirmed by the orthorhombic distortion that is similar to ICDD #98-8636. A small amount of $Bi_{12}TiO_{20}$ phase was found in the sample prepared at pH 3, which is attributed to the existence of excessive Bi^{3+} ions. This result agrees with the presence of the (3 1 0) peak in the XRD pattern. Besides, the unit cell volume was found to shrink at higher pH values, due to the unit cell distortion. The results indicate that the increase in OH^- content and the formation of NH_4NO_3 prohibited the formation of an inorganic substance containing Ti–O groups, and simultaneously favor the formation of the TiO_6 octahedron.

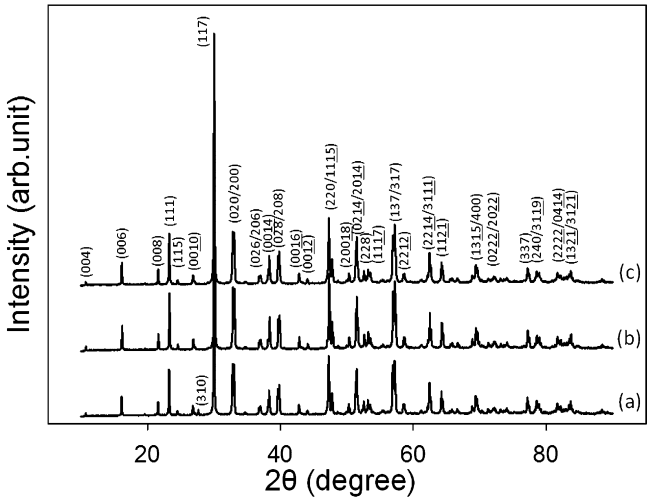

Fig. 4. XRD patterns of the BIT powders prepared at (a) pH 3, (b) pH 5 and (c) pH 7.

To verify the influence of pH on the structure change, Raman analysis was conducted, and the results are shown in Fig. 5. The result shows the presence of 13 Raman active modes. The peak intensity tended to increase as increasing the pH value, predominantly at the low wavenumbers. The splitting of the peak at 269 and 227 cm^{-1} was observed from the sample prepared at pH 3 and 5 (Fig. 5b and c). This pointed out the formation of the $Bi_4Ti_3O_{12}$ phase with an orthorhombic symmetry and the *Fmmm* space group [30], as confirmed by the

Table 1
Refinement indexes of the BIT powders prepared at different pH values.

Parameter	ICDD	pH 3	pH 5	pH 7
Refinement indexes				
Space group	*Fmmm*	*Fmmm*	*Fmmm*	*Fmmm*
R_{exp}(%)	–	4.549	4.421	4.392
R_p(%)	–	10.169	10.228	10.157
R_{wp}(%)	–	11.628	11.992	11.731
S	–	2.56	2.71	2.67
Unit cell parameters				
a(Å)	5.410	5.408	5.408	5.408
b(Å)	5.448	5.445	5.444	5.446
c(Å)	32.830	32.809	32.812	32.814
Unit cell distortion	1.0070	1.0068	1.0066	1.0070
Unit cell volume (Å^3)	–	965.979	966.341	966.067
Weight fraction (%)	–	96.43	100	100

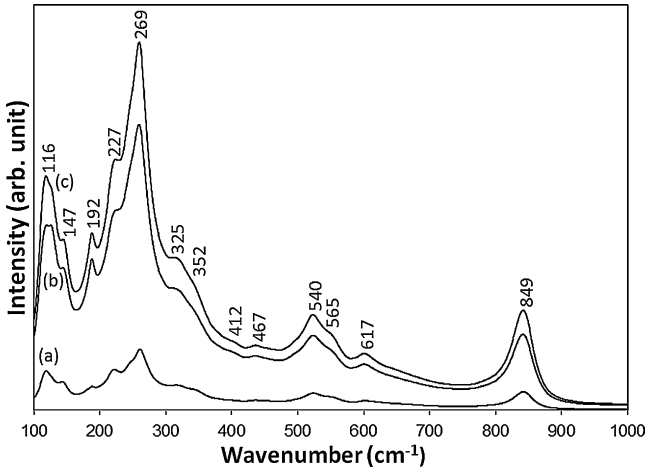

Fig. 5. Raman spectra of the BIT powders prepared at (a) pH 3, (b) pH 5 and (c) pH 7.

presence of the split modes at 227 and 192 cm^{-1} and 540 and 565 cm^{-1}. The predominant modes positioned at 269, 540 and 849 cm^{-1} are attributed to the presence of perovskite structure [6]. The intense mode intensity at higher pH value indicates that high OH^- ion content favored the formation of the TiO_6 octrahedron. In addition, a Raman mode at 849 cm^{-1} is primarily attributed to the symmetry of the Ti–O stretching vibration in the TiO_6 octahedron, which is symmetrical with the mode at 617 cm^{-1}. The Raman modes at 269, 325, 540, 617 and 849 cm^{-1} corresponded to the internal vibration mode of the TiO_6 octahedron [31]. Two modes at 540 and 565 cm^{-1} are related to the opposing excursions of the external apical oxygen atoms of the TiO_6 octahedron [32], which reveals the doubly degenerate symmetry of the O–Ti–O stretching vibration mode. The combination of the splitting modes at 269 and 227 cm^{-1} corresponded to a weak bending vibration of O–Ti–O in the TiO_6 octahedron. The result showed the increase in the TiO_6 octahedron distortion at high pH value, resulting in a higher unit cell distortion, as shown in Table 1. This is confirmed by the increase in the peak intensity of the modes at 325, 540, 617 and 849 cm^{-1} and the splitting of the modes at 227 and 192 cm^{-1}, and 540 and 565 cm^{-1} [33]. The larger distortion in the TiO_6 octahedron is due to a strong hybridization between Bi6s and O2p orbitals caused by an addition OH^- [9]. This is manifested by the increased peak intensity of the active mode at 116 cm^{-1}. Thus, it can be concluded that more OH^- ions can stabilize the H^+ ions in the TiO_6 octahedron, and consequently contribute a stronger hybridization of Bi–O.

Besides the phase formation, the pH value of the initial precursor was also found to affect the morphology of the BIT powder. A hard agglomeration of a large, plate-like morphology with an average particle size of approximately 10–20 μm was observed from the powder prepared under strong acidic conditions (Fig. 6a). With increasing pH value, the formation of large late-like structure was found to decrease. Furthermore, it exhibited a soft agglomeration with the particle size in the range of 10–20 μm (Fig. 6b and c).

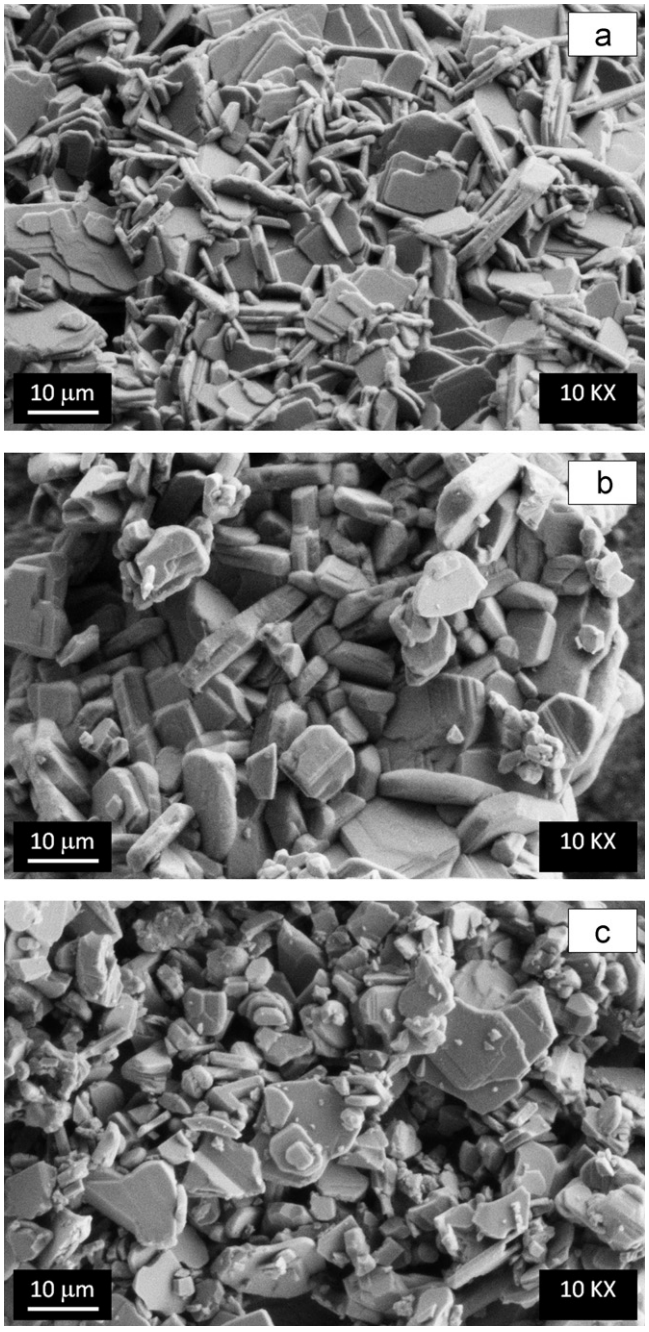

Fig. 6. Morphologies of the BIT powders prepared at (a) pH 3, (b) pH 5 and (c) pH 7.

The powder obtained from the neutral condition (pH 7) demonstrated a soft agglomeration with the particle size in the range of 2–15 μm (Fig. 6c). A hard agglomeration of particles prepared in acidic conditions is due to the explosion of Ti–OH in the precursor that contained a large amount of H^+ ions. This led to a high content of the deprotonated ($Ti–O^-$) hydroxyl group, and thus resulted in strong attractive force between the particles. The addition of the OH^- ions generated protonated ($Ti–OH_2^+$) hydroxyl groups, which reduced the attractive force between the particles [34], and thus resulted in a soft agglomeration.

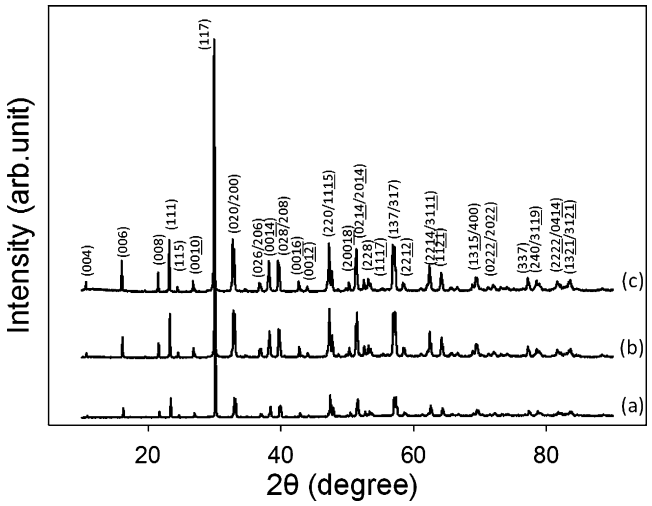

Fig. 7. XRD patterns of the BIT ceramic prepared at (a) pH 3, (b) pH 5 and (c) pH 7.

3.2. Ceramics fabrication

The presence of the $Bi_4Ti_3O_{12}$ phase was found in the ceramics prepared at all of the pH conditions after being subjected to sintering at 1150 °C for 3 h (Fig. 7), revealed a stability of the $Bi_4Ti_3O_{12}$ phase (ICDD #98-8636). This is attributed to the suppression of the independent volatility of O near Bi^{3+} via a stronger hybridization Bi–O [26], as verified by the Raman analysis result (Fig. 5). It is notable that the $Bi_{12}TiO_{20}$ phase in the sample prepared at pH 3 was not detected. This is probably due to the volatility of the $Bi_{12}TiO_{20}$ phase at the temperature higher than 875 °C [35]. The stronger and sharper XRD peak was found in the ceramic prepared at the higher pH value, indicating the crystal growth after subjected to sintering (Table 2).

The refinement results reveal the formation of the $Bi_4Ti_3O_{12}$ phase in the ceramics prepared at all of the conditions. The BIT phase with an orthorhombic structure and the unit cell parameters of a = 5.407 Å, b = 5.445 Å and c = 32.839 Å were obtained from the ceramic prepared at pH 7 condition. Furthermore, the unit cell distortion (1.00707) was found to have a slight deviation, as compared to the ICDD database. Besides, the crystallite size was found to increase with increasing pH value, as conformed to the stronger XRD peak intensity (Fig. 7). Thus, it can be concluded that a BIT ceramic can be prepared using low-temperature self-combustion at a neutral condition without any additional Bi^{3+}. This result is different from those reported in the literatures, which have stated the essential of the additional Bi^{3+} on the formation of $Bi_4Ti_3O_{12}$ phase [36,37].

Table 2
Refinement indexes of the BIT ceramics prepared at different pH values.

Parameter	ICDD	pH 3	pH 5	pH 7
Refinement index				
Space group	*Fmmm*	*Fmmm*	*Fmmm*	*Fmmm*
R_{exp}(%)	–	7.939	8.036	8.604
R_p(%)	–	26.760	25.563	24.155
R_{wp}(%)	–	30.393	27.807	27.326
S	–	3.83	3.46	3.18
Unit cell parameters				
a(Å)	5.410	5.406	5.406	5.407
b(Å)	5.448	5.445	5.444	5.445
c(Å)	32.830	32.846	32.849	32.839
Unit cell distortion	1.00702	1.00712	1.00709	1.00707
Crystallite size (nm)	–	162.05	191.49	217.54
Unit cell volume (Å^3)	–	966.885	966.698	966.679
Weight fraction (%)	–	100	100	100

Ceramic prepared under a strong acidic condition (pH 3) exhibited a low relative density as low as 83%. The relative density was found to increase to 88.80% and 91.35% from those prepared at weak acidic (pH 5) and neutral (pH 7) conditions. A low relative density is caused by a large anisotropic grain growth, which resulted in large plate-like particles (see in Fig. 6a). This is verified by the presence of a large grain size in the range of 5–20 μm (Fig. 8a), as compared to those prepared at weak acidic or neutral conditions (Fig. 8b and c). Such features resulted in the formation of pores in the triple-junctions (inset in Fig. 8a). This may be associated by the independent volatility of Bi^{3+} caused by the weak hybridization of Bi–O. The enhanced relative density of a ceramic prepared at neutral condition is due to the formation of homogeneous anisotropic grains with the grain size in the range of 2–10 μm (Fig. 8c). Furthermore, it is favored by the existence of fine grains between the triple-junctions (inset in Fig. 8c). Other than that, the stronger hybridization of Bi–O also contributed to the reduction of porosity by the suppression of the independent volatility of Bi^{3+}. This can be restricted the crystal growth by the reduction of oxygen vacancy.

Fig. 9 illustrates the dielectric constant (ε) and dissipation factor (tan δ) at room temperature of the BIT ceramics prepared at different pH values as a function of frequency in the range of 10 Hz to 1 MHz. In dielectric materials, four types of polarization, such as electronic polarization (ε_e), ionic polarization (ε_i), dipolar polarization (ε_d) and space charge polarization (ε_s) contribute to the ε. Theoretically, the frequencies for ε_e and ε_i are approximately 10^{16} and 10^{13} Hz, respectively [38]. This reveals that the dielectric properties in this work are predominantly contributed from ε_s and ε_d. It is well known that the pristine BIT possesses a certain amount of inherent defects, e.g. O^{2-} vacancies caused by the volatility of Bi and Bi_2O_3 at high temperatures [9]. The O^{2-} vacancies consequently act as space charge, and thus dramatically induce the conductivity up on increasing frequency [39]. Based on this basis, it affirms the presence of O^{2-} vacancies in all samples, as shown by the reduction of ε (Fig. 9a). However, the results show that the ceramic prepared at pH 7 retains smaller number of O^{2-} vacancies. This is manifested by the relatively lower reduction rate of ε (12.3%), as compared to those prepared at pH 5 (14.0%) and pH 3 (17.1%). Moreover, the reduced O^{2-} vacancies in ceramics prepared at higher pH values also contributed to the drastic increase in the ε, and reached a maximum of approximately 340 for that prepared at pH 7. This is due to a strong hybridization of Bi–O, as discussed earlier.

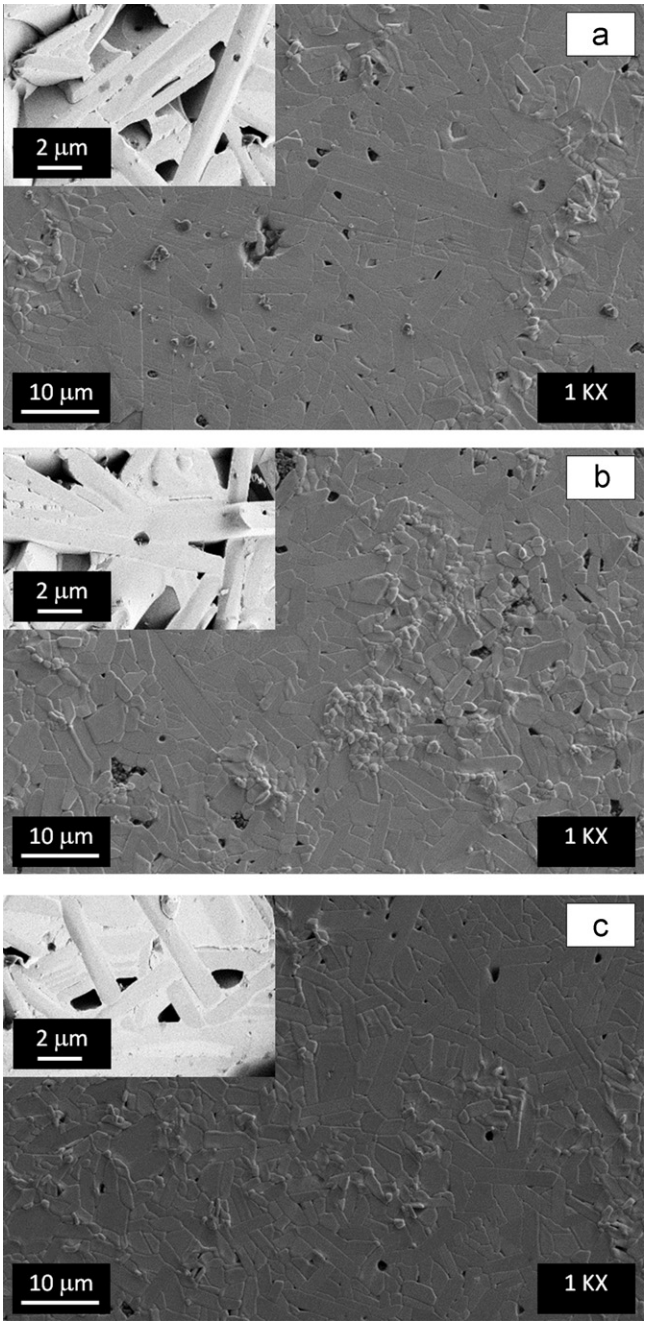

Fig. 8. Morphologies of the BIT ceramics prepared at (a) pH 3, (b) pH 5 and (c) pH 7. Inset shows the fracture surface at a 5kX magnification.

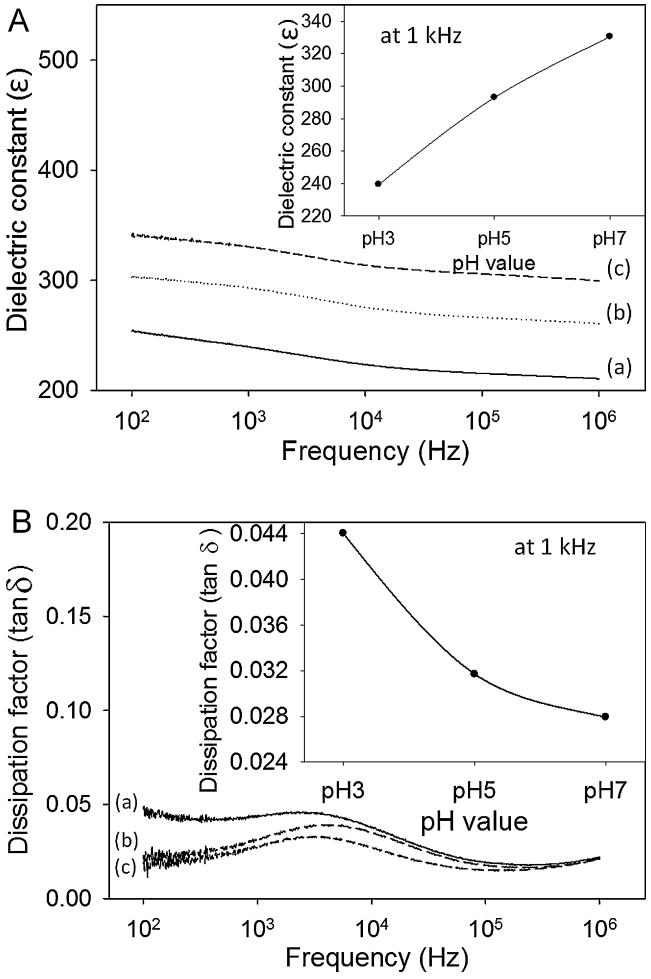

Fig. 9. [A] Dielectric constant and [B] dissipation factor of the BIT ceramics prepared at (a) pH 3, (b) pH 5 and (c) pH 7. Insets show those at 1 MHz.

Besides that, the microstructure of ceramics also plays a crucial role to determine the ε value through the number of ε_d. The increased ε in the samples prepared at high pH values is caused by the decrease in the grain size. The 90° domain arrangements can be formed in microstructure that is composed of the grain sizes in the range of 1–10 μm, whereas the microstructure with the grain size bigger than 10 μm allows the formation of both 90° and 180° domain arrangements. The twinning through the formation of both the 90° and 180° domains arrangement induced three-dimension compensation, and the relaxation of internal stress [40]. This leads to the reduction of the ε, as verified by the result obtained from ceramic prepared at pH 3. On the other hand, the 90° domain density also greatly influences the ε. The number of 90° domains per grain therefore decreased with grain size, resulting in larger unrelieved stresses, and thus contributed to a higher ε [40,41]. This is confirmed by the increased ε in the ceramic prepared at pH 7 that is composed a fine grain size in the range of 1–10 μm. This allowed the formation of the 90° domains arrangement with a high domain density, which retained a high internal stress, and thus resulted in higher ε [42]. In Fig. 9b, the decrease in tan δ is observed from the ceramics prepared at higher pH values. The reduced tan δ is greatly attributed to the reduction of space charge polarization by the minimum O^{2-} vacancies, which is in agreement with literatures [38,39]. Other than that, a minimum grain defect in the ceramic with a low volatility also contributed to the accomplishment of ceramic with a low tan δ (~0.028), owing to a minimum electric flux continuity between grains [43].

In order to predict the maximum operation temperature of the BIT ceramic, a ceramic produced under pH 7 condition was subjected to the temperature dependent dielectric measurement under different frequencies. Fig. 10 clearly shows that the ε increased drastically upon increasing temperature, while it decreased linearly with increasing frequency. The increased ε at a

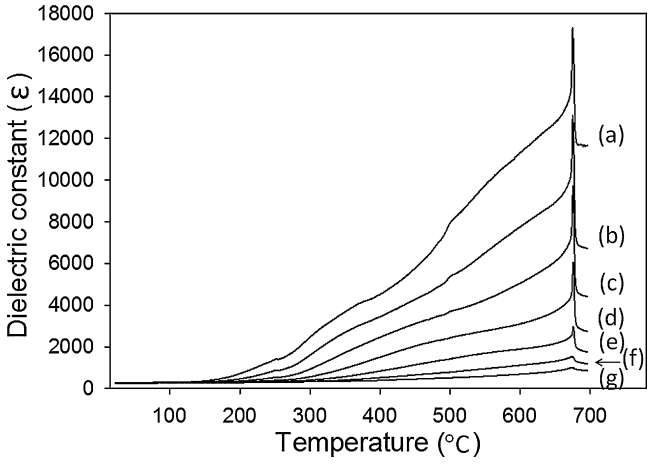

Fig. 10. Variation of dielectric constant with temperature measured at frequency of (a) 1 kHz, (b) 3 kHz, (c) 10 kHz, (d) 30 kHz, (e) 100 kHz, (f) 300 kHz and (g) 1 MHz.

high temperature is due to the high polarization process [44]. The reduction in ε at higher frequencies is caused by the presence of O^{2-} vacancies. The O^{2-} vacancies would induce new energy levels in the band gap, and thus led to a higher conductivity [39]. From the finding, the ε increased continuously with increasing temperature, and it decreased abruptly at approximately 675 °C. This dielectric constant transition is well-known as Curie temperature (T_c) [38], indicating the possibility to use this material for high temperature application up to 675 °C. This value is precisely same with standard T_c value of 675 °C [1–4], and better than those produced by co-precipitation synthesis [7], as well as self-propagation combustion synthesis [13]. The result indicates the remarkable capability of this alternative method to produce high purity BIT ceramic for the use in high temperature applications.

4. Conclusions

The pH value of the initial precursor greatly influences the formation and properties of BIT ceramics prepared via a low-temperature self-combustion synthesis. The addition of an NH_4OH solution in the nitrate precursor favored the combustion by the formation of an intermediate fuel, NH_4NO_3. Moreover, higher number of OH^- ions induced the deceleration of the vaporization, and higher decomposition rate, and thus in turn to the formation of soft agglomeration BIT particles. It simultaneously restricted the independent volatility of Bi and Bi_2O_3. Such conditions are able to control the phase formation and microstructure of BIT, which resulted in the enhancement of the dielectric properties. In conclusion, the BIT ceramic prepared via the low-temperature self-combustion method at the neutral condition offered better properties, as compared to those prepared in acidic conditions.

Acknowledgements

The authors gratefully acknowledge Prof. Yuji Noguchi, Institute of Industrial Science, The University of Tokyo for his help in dielectric measurement and valuable opinion. This also extends the ASEAN University Network for Science and Engineering Education (AUN/SEED-net) (6050151) for financial support.

References

[1] B. Aurivillius, Mixed bismuth oxides with layers lattices; II, Structure of $Bi_4Ti_3O_{12}$, Arkiv. fur. kemi. 1 (1949) 499–512.
[2] K.R. Chakraborty, S.N. Achary, S.J. Patwe, P.S.R. Krishna, A.B. Shinde, A.K. Tyagi, Low temperature neutron diffraction studies on $Bi_4Ti_3O_{12}$, Ceram. Int. 33 (2007) 601–604.
[3] S.H. Hong, T.-M. Susan, L.M. Gary, Dielectric and ferroelectric properties of Ta-doped bismuth titanate, J. Mater. Sci. Lett. 19 (2000) 1661–1664.
[4] T. Jardiel, A.C. Caballero, M. Villegas, Aurivillius ceramics: $Bi_4Ti_3O_{12}$-based piezoelectric, J. Ceram. Soc. Jpn. 116 (2008) 511–518.
[5] Z.Z. Lazarevic, N.Z. Romcevic, J.D. Bobic, M.J. Romcevic, Z. Dohcevic-Mitrovic, B.D. Stojanvic, Study on bi-layered ceramics powders prepared by the mechanochemical, J. Alloys Compd. 486 (2009) 848–852.
[6] J. Hou, R.V. Kumar, Y. Qu, D. Krsmanovic, Controlled synthesis of photoluminescent $Bi_4Ti_3O_{12}$ nanoparticles from metal-organic polymeric precursor, J. Nanopart. Res. 12 (2009) 563–571.
[7] Z.-H. Chen, J.-F. Qiu, C. Liu, J.-N. Ding, Y.-Y. Zhu, Preparation of $Bi_4Ti_3O_{12}$ nanopowder by azeotropic co-precipitation and dielectric properties of the sintered ceramic, Ceram. Int. 36 (2010) 241–244.
[8] Z. Chen, G. Zhao, H. Li, G. Han, Effects of water amount and pH on the crystal behavior of a TiO_2 nanocrystalline derived from a sol–gel process at a low temperature, J. Am. Ceram. Soc. 92 (2009) 1924–1929.
[9] J.C. Bae, S.S. Kim, E.K. Choi, T.K. Song, Ferroelectric properties of lanthanum-doped bismuth titanate thin films grown by a sol–gel method, Thin Solid Films 472 (2005) 90–95.
[10] X. Du, Y. Xu, H. Ma, J. Wang, X. Li, Synthesis and characterization of bismuth titanate by an aqueous sol–gel method, J. Am. Ceram. Soc. 90 (2007) 1382–1385.
[11] H. Miao, M. Dong, G. Tan, Y. Pu, Z. Sun, Hydrothermal preparation of bismuth titanate nanopowders, Key Eng. Mater. 336–338 (2007) 161–164.
[12] A.Z. Simoes, B.D. Stojannovic, M.A. Zaghete, C.S. Riccardi, A. Ries, F. Moura, E. Longo, J.A. Varela, Electrical characterization of Lanthanum-modified bismuth titanate thin films obtained by the polymeric, J. Integr. Ferroelectr. 60 (2004) 21–31.
[13] Z.S. Macedo, C.R. Ferrari, A.C. Hernandes, Impedance spectroscopy of $Bi_4Ti_3O_{12}$ ceramic produced by self-propagating high-temperature synthesis technique, J. Eur. Ceram. Soc. 24 (2004) 2567–2574.
[14] K.C. Patil, M.S. Hegde, T. Rattan, S.T. Aruna, Chemistry of Nanocrystalline Oxide Materials: Combustion Synthesis, Properties and Applications, World Scientific Publishing Co. Pte. Ltd., Singapore, 2008 , pp. 1–58.
[15] C.-H. Han, H.S. Lee, S.D. Han, Synthesis of nanocrystalline TiO_2 by sol–gel combustion hybrid method and its application to dye solar cells, Bull. Korean Chem. Soc. 29 (2008) 1495–1498.
[16] R. Zhang, J. Huang, J. Zhao, Z. Sun, Y. Wang, Sol–gel auto-combustion synthesis of zinc ferrite for moderate temperature desulfurization, Energy Fuels 21 (2007) 2682–2687.
[17] M. Jacquin, Y. Jing, V. Essoumhi, G. Taillades, D.J. Jones, J. Rozière, Flash combustion synthesis and characterisation of nanosized proton conducting yttria-doped barium cerate, J. New Mater. Electrochem. Syst. 10 (2007) 243–248.
[18] H.M. Xu, H.G. Yan, Z.H. Chen, Low-temperature combustion synthesis and sintering of nanosized $Ce_{0.8}Y_{0.2}O_{1.9}$ powders, Mater. Charact. 59 (2008) 301–305.
[19] J. Chandradass, K.K. Hyeon, Synthesis and characterization of $LaAlO_3$ nanopowders by emulsion combustion method, J. Alloys Compd. 481 (2009) 3–18.
[20] S. Luo, Z. Tang, W. Yao, Z. Zhang, Low-temperature combustion synthesis and characterization of nanosized tetragonal barium titanate powders, Microelectron. Eng. 66 (2003) 147–152.

[21] T. Thongtem, S. Thongtem, Characterization of $Bi_4Ti_3O_{12}$ powder prepared by the citrate and oxalate co-precipitation processes, Ceram. Int. 30 (2004) 1463–1470.
[22] A.V. Prasadarao, A.I. Robin, S. Komarneni, Bismuth titanate from nanocomposite and sol–gel processes, Mater. Lett. 28 (1996) 469–473.
[23] H. Gu, W. Cao, R. Song, X. Zhou, J. Wang, Effect of precursor solution pH value and substrate texture on orientation degree of sol–gel-derived bismuth titanate thin films, Phys. Stat. Sol. (a) 198 (2003) 282–288.
[24] K.H. Wu, C.H. Yua, Y.C. Chang, D.N. Horng, Effect of pH on the formation and combustion process of sole-do auto-combustion derived NiZn ferrite/SiO_2 composites, J. Solid State Chem. 177 (2004) 4119.
[25] S.C. Roy, G.L. Sharma, M.C. Bhatnagar, R. Manchanda, V.R. Balakrishnan, S.B. Samanta, Effect of pH on electrical and optical properties of sol–gel derived microcrystalline $Ba_{0.5}Sr_{0.5}TiO_3$ thin films, Appl. Surf. Sci. 236 (2004) 306–312.
[26] A.Z. Simoes, A. Ries, F. Moura, C.S. Riccardi, E. Longo, J.A. Varela, Influence of the solution pH on the morphological, structural and electrical properties of $Bi_{3.50}La_{0.50}Ti_3O_{12}$ thin films obtained by the polymeric precursor method, Mater. Lett. 59 (2005) 2759–2764.
[27] U. Chon, J.S. Shim, Ferroelectric properties and crystal structure of praseodymium-modified bismuth titanate, J. Appl. Phys. 93 (2003) 4769–4775.
[28] A.M. Umabala, M. Suresh, A.V. Prasadarao, Bismuth titanate from coprecipitated stoichiometric hydroxide precursors, Mater. Lett. 44 (2000) 175–180.
[29] E.C. Subbarao, Ferroelectricity in $Bi_4Ti_3O_{12}$ and its solid solutions, Phys. Rev. 122 (1961) 804–807.
[30] P.R. Graves, G. Hua, S. Myhra, J.G. Thompson, The Raman modes of the Aurivillius phase: temperature and polarization dependence, J. Solid State Chem. 114 (1995) 112–122.
[31] Z.Z. Lazarevic, B.D. Stojanvic, C.O. Paiva-Santos, N.Z. Romcevic, Study of structure and properties of $Bi_4Ti_3O_{12}$ prepared by mechanochemical syntheses, Ferroelectrics 368 (2008) 154–162.
[32] Y.L. Du, M.S. Zhang, Q. Chen, Z.R. Yuan, V. Yin, Q.A. Zhang, Size effect and evidence of a size-driven phase transition in $Bi_4Ti_3O_{12}$ nanocrystals, Solid State Commun. 124 (2002) 113–118.
[33] Y. Wang, G. Xu, X. Zhang, W. Tang, G. Cheng, Y. Zhu, Structural and optical properties of $Bi_{4-x}Nd_xTi_3O_{12}$ thin films prepared by metal-organic solution deposition, Mater. Lett. 58 (2004) 813–816.
[34] B. Ohtani, Y. Okugawa, S.-I. Nishimoto, T. Kagiya, Photocatalytic activity of TIO, powders suspended in aqueous silver nitrate solution: correlation with pH-dependent surface structures, J. Phys. Chem. 91 (1987) 3550–3555.
[35] S.P. Yordanov, Ch.P. Carapanov, I.S. Ivanov, P.T. Cholakov, Dielectric properties of the ferroelectric $Bi_2Ti_3O_9$ ceramics, Ferroelectrics 209 (1998) 541.
[36] M. Yamada, N. Iizawa, T. Yamaguchi, W. Sakamoto, K. Kikuta, T. Yogo, T. Hayashi, S.-I. Hirano, Processing and properties of rare earth ion-doped bismuth titanate thin films by chemical solution deposition method, Jpn. J. Appl. Phys. 42 (2003) 5222–5226.
[37] C.P. Cheng, M.H. Tang, Z. Ye, X.L. Zhong, X.J. Zheng, Y.C. Zhou, Z.S. Hu, Structure evolution and ferroelectric properties of $Bi_{3.4}Yb_{0.6}Ti_3O_{12}$ thin films crystallized under moderate temperature, Mater. Lett. 61 (2007) 3563–3566.
[38] I. Coondoo, A.K. Jha, S.K. Agarwal, Structural, dielectric and electrical studies in tungsten doped $SrBi_2Ta_2O_9$ ferroelectric ceramics, Ceram. Int. 33 (2007) 41–47.
[39] A.Z. Simoes, R.F. Pianno, C.S. Riccardi, L.S. Cavalcante, E. Longo, J.A. Varela, Dielectric properties of pure and lanthanum modified bismuth titanate thin films, Ceram. Int. 454 (2008) 66–71.
[40] G. Arlt, Microstructure and domain effects in ferroelectric ceramics, Ferroelectrics 91 (1989) 3–7.
[41] L.B. Kong, J. Ma, W. Zhu, O.K. Tan, Preparation of $Bi_4Ti_3O_{12}$ ceramics via a high-energy ball milling process, Mater. Lett. 51 (2001) 108–114.
[42] W.R. Buessem, L.E. Cross, A.K. Goswami, Phenomenological Theory of high permittivity in fine-grained barium titanate, J. Am. Ceram. Soc. 49 (1996) 33–36.
[43] K.W. Gachigi, U. Kumar, J.P. Dougherty, Grain Size Effect in Barium Titanate. ISAF' 92, in: Proc. Eighth IEEE Int. Symp. Appl., 2002, 492–495.
[44] M. Raghavender, G.S. Kumar, G. Prasad, Modification of dielectric relaxations in sodium bismuth titanate with samarium doping, J. Phys. Chem. Solids 67 (2006) 1803–1808.